ABUAD Journal of Engineering Research and Development (AJERD)
ISSN (online): 2645-2685; ISSN (print): 2756-6811

Volume 7, Issue 1, 260-277

L-Index-Based Technique for Voltage Collapse Prediction and Voltage Stability Enhancement in Electrical Power Systems

Akintunde Samson ALAYANDE[1], Amirah Opeyemi HASSAN[1], Flourish OLOBANIYI[1], Samuel Olufemi OSOKOYA[2], Azeez Ishola ADEBESHIN[3], Ayoade Benson OGUNDARE[3]

[1]*Department of Electrical and Electronics Engineering, University of Lagos, Nigeria*
aalayande@unilag.edu.ng/amirahhassan93@gmail.com/folobaniyi@unilag.edu.ng

[2]*Department of Electrical and Electronics Engineering, Yaba College of Technology, Nigeria*
sosokoya@yahoo.com

[3]*Department of Electrical and Electronics Engineering, Lagos State University of Science and Technology, Ikorodu*
Azeezalex@yahoo.com/ayoadebensonoludare@yahoo.com

Corresponding Author: aalayande@unilag.edu.ng, *+2347036771333*
Date Submitted: 06/01/2024
Date Accepted: 26/05/2024
Date Published: 05/06/2024

Abstract: *Recent years have witnessed a notable increase in the occurrence of blackouts, especially in developing nations, attributed to the continuously growing demand on modern power networks. Given that the demand shows no signs of abating and is projected to increase further in the coming years, additional research on power system stability is imperative. This study, therefore, investigates voltage stability assessment in power systems using the L-index methodology, focusing on the Nigerian 28-bus system and the IEEE system. The L-index offers a practical means of identifying weak buses and evaluating voltage stability margins. Calculating L-index values for load buses under diverse conditions identifies critical points, with higher values indicating vulnerability. The research investigates injecting reactive power at load buses to prevent collapse, comparing outcomes with and without compensation. Analyzing the L-index's performance across varied loading scenarios confirms its precision in predicting breakdown points and identifying critical buses. Load flow analysis of the Nigerian 28-Bus system reveals that only bus 16 exceeds voltage limits, while line analysis shows total power losses. Increasing loadability exposes bus 16 as the weakest, supported by its low voltage magnitude. The research confirms bus 16 as the system's weakest point, guiding corrective measures to enhance stability and prevent collapse. Utilizing Matlab for implementation, this study contributes valuable insights into system vulnerability and provides a framework for improving voltage stability in power systems.*

Keywords: *Voltage Collapse, Voltage Collapse Prediction, Voltage Stability, L-index, Static Synchronous Compensator (STATCOM), Voltage Stability Enhancement.*

1. INTRODUCTION

Voltage collapse has emerged as a significant challenge for electric power companies worldwide in recent times [1, 2]. It is a critical issue in power system operation and planning, characterized by a gradual decline in system voltage. The ever-increasing demand for electricity from consumers has led to a rapid increase in the complexity of modern power systems. This complexity places additional stress on the system, rendering it more susceptible to voltage instability and, ultimately, voltage collapse [3, 4]. Notably, emerging nations have experienced significant blackouts in recent years due to the continuous rise in demand on contemporary power networks. As the demand shows no signs of slowing down and is anticipated to increase further in the coming years, it becomes imperative to conduct additional research on power system instability.

The prevailing trend towards a competitive business environment has compelled modern utilities to optimize available resources. Consequently, today's power systems face heightened burdens due to increasing demand, the pursuit of maximum economic benefits, and efficient utilization of transmission capacity [5, 6]. The more efficient utilization of the transmission network has resulted in many power systems operating closer to voltage stability limits, thereby elevating the risk of voltage collapse. In such delicate circumstances, even minor disturbances can jeopardize system security and lead to voltage decline [7]. Therefore, there is an urgent need for a predictive method that can assess the voltage security level of a given operational situation and alert the system operator to take necessary preventive actions.

Although the existing methods have contributed in no small measures as regard voltage collapse detection in power systems, there are still unsolved issues associated with those method. For example, Fast Voltage Stability Index (FVSI) may not capture long-term stability issues or consider the effects of large disturbances on the system. Voltage Stability (Lp)

Index may require extensive computational resources for large power systems. Voltage Stability Load Bus Index (VSLBI) may require detailed modeling of load characteristics and may not capture a wide range of voltage stability issues. The L-Index stands out as a superior measure of voltage collapse prediction for several reasons. Unlike other indices, the L-Index directly measures the proximity to voltage collapse by considering the distance to the nearest saddle-node bifurcation point. This provides a clear indication of how close the system is to instability. Additionally, the L-Index is computationally efficient, making it suitable for large power systems. While other indices offer valuable insights, the L-Index's direct and efficient approach makes it a preferred choice for voltage collapse prediction. The L-Index emerges as a better measure of voltage collapse prediction compared to other methods. Its direct measurement of proximity to voltage collapse and computational efficiency makes it a valuable tool for assessing system stability and guiding corrective actions. By leveraging the advantages of the L-Index, power system operators can better anticipate and mitigate voltage instability, thereby enhancing grid reliability and resilience. In this study, L-index-based technique is employed, which measures the distance from the current operating point to the nearest saddle-node bifurcation point on the voltage stability boundary. Its main advantage is that it provides a direct measure of the proximity to voltage collapse and is computationally efficient for large power systems. The traditional L-index-based approaches usually assume a static system model. As such, dynamic stability issues remain unsolved. However, this bottleneck is overcome in this work as the dynamic system operational loadings are captured, which also takes into account accurate system parameters that may be sensitive to modeling uncertainties. In this context, this study aims to assess the effectiveness of the L-index methodology in predicting voltage collapse in modern power systems. The L-index is a stability index that considers both static and dynamic aspects of voltage stability, making it a promising candidate for accurately assessing the proximity of voltage collapse. By leveraging the capabilities of the L-index and incorporating advanced modelling techniques, such as the inclusion of STATCOM devices, we seek to improve the accuracy and reliability of voltage collapse prediction. Specifically, this study investigates the capability of the L-index to foresee the proximity of voltage collapse in a real-world power system scenario, focusing on the IEEE 30-bus system and the Nigerian 330 kV, 28-bus system as case studies. By comparing the performance of the L-index with existing methods and evaluating the impact of STATCOM devices on system stability, we aim to provide insights into the effectiveness of the proposed approach in addressing the challenges posed by voltage collapse.

The structure of this paper is as follows: Section 2 presents an extensive review of literature while the mathematical formulation of the L-index technique starting from the theoretical framework and its application in voltage collapse prediction is presented in section 3. In section 4, we first described, in brief, the case studies considered, which include the IEEE 30-bus system and the Nigerian 330 kV, 28-bus system, highlighting the key features of each system. The results of the analysis as well as discussion of the findings are also presented in section 4. Finally, the paper is concluded in section 5, summarizing the main contributions. The directions for future researches are also outlined in this section.

2. EXTENSIVE LITERATURE REVIEW

Several authors have contributed to the effort of accurately predicting voltage collapse in a system. For example, in the study presented in reference [8], a new forecasting technique is introduced to anticipate the voltage stability class label based on a suggested classification approach. The model integrates Hopf and limits driven bifurcations and utilizes an information theoretic feature selection method, an extreme learning machine (ELM) as the forecast engine, and a line search procedure to fine-tune parameters. The effectiveness of the proposed classification model and prediction method is demonstrated using the New England 39-bus and IEEE 145-bus test systems. Compared to previous artificial intelligence-based approaches, this method provides more accurate stability class labels with reduced computational effort, enabling quick and precise determination of voltage stability states in unknown situations. In the study carried out in [9], the authors present a unique technique based on data mining and machine learning for instantaneous evaluation of short-term voltage stability (STVS) under significant disruptions. The method employs the calculation of the maximal Lyapunov exponent and dynamic voltage indices to classify the stability of the power system in different operational modes offline. A machine learning algorithm, specifically a Random Forest, is trained on the processed multivariate time series data of the power system's dynamic response to categorize the post-disturbance functioning state in real-time, detecting both quick voltage collapses and fault-induced delayed voltage recovery events. In [10], the authors proposed an active learning approach to enhance the usefulness of machine learning in power system prediction. The method continuously interacts with the offline training and online prediction processes, identifying operational points where machine learning predictions diverge from actual system conditions. By structuring the training set around these acknowledged operational points, the capacity of machine learning algorithms to predict impending power system conditions is improved. Additionally, the approach minimizes the number of simulations on a complex power system model, expediting the offline training process. However, drawbacks include significant training time, prediction time, and the number of measurements required to achieve high prediction accuracy. In [11], the authors proposed a unique method for forecasting the voltage collapse point using the quadratic line voltage stability index (q-LVSI) and auditory machine intelligence (AMI). The method is applied to a subset of buses in the 330kV-30bus power network in Nigeria. To validate the proposed method, it is compared to the Group Method of Data Handling for Time Series (GMDH Time-Series), a polynomial function fitting neural network based on inductive learning and self-organization. Simulation tests show that the AMI procedure is competitive with the GMDH time-series method in terms of performance. In [12], the authors present methods for estimating the severity of voltage collapse contingencies under uncertainty and demonstrate their application in the French EHV network for ranking potential risks. The research highlights the importance of incorporating the original characteristics of past load distributions

to achieve accurate assessments. Two likelihood severity estimation approaches, standard and generalized, are developed to account for the correlation and nature of the probability distribution of the multivariate load parameter representing uncertainty in operating conditions. Accurate severity estimation is achieved with reduced computing effort using linear sensitivities and machine learning algorithms. The linear sensitivities are computed by sampling different load stress directions from the multivariate load parameter state space using the Latin Hypercube Sampling (LHS) approach. The proposed concepts are demonstrated on the French network using seven significant contingencies, and the severity estimations are validated for accuracy and computing efficiency through full-fledged contingency simulation.

In [13], the authors proposed an online forecast technique for short-term voltage stability (STVS) based on long short-term memory networks (LSTM) and graph convolutional networks (GCN). They introduce GCN-LSTM, a novel machine learning framework that combines GCN to capture spatial aspects and LSTM to capture temporal aspects of power grids. The proposed technique utilizes the GCN-LSTM model for STVS online forecasting, capable of predicting STVS results and multiplexing spatial-temporal STVS evolution trends. The method is tested on a modified 39-bus system and a 68-bus system as case studies, using training and test data generated by the Power System Simulator/Engineering (PSS/E). Simulation results demonstrate the high efficiency of the suggested method. In [14], the authors proposed an approach for online assessment of the voltage stability margin (VSM) using an optimal fuzzy system and feature selection method. The technique performs well for large power systems and consists of three main components: feature extraction and selection, estimation, and training. The association rules (AR) technique is used to select the most efficient loading parameters, which serve as the input to the adaptive neuro-fuzzy inference system (ANFIS) for VSM estimation. The ANFIS is trained effectively using the Harris Hawks Optimization Algorithm (HHOA). The suggested method allows for accurate online monitoring of VSM in both small and large systems, enabling the application of relevant control measures to prevent voltage collapse. MATLAB simulations demonstrate that the proposed technique outperforms previously presented VSM assessment methodologies. The technique is tested on the 39-bus, 118-bus, and 300-bus IEEE test systems. In [15] the authors present a new technique for identifying load buses that are close to voltage collapse by evaluating the static voltage stability of load buses under given operating conditions. The voltage equation of a two-bus network is used to create the Thevenin equivalent circuit of the load bus, from which a voltage stability index, known as the L-index, is derived. Artificial neural networks and the Newton Raphson load flow method are used to calculate the L-index. This method helps identify weak points in the system that require significant reactive power support, with the bus having the highest L-index value indicating the most vulnerable bus in the system. The technique is evaluated using the IEEE-14 bus test system. In [16], the authors proposed the use of artificial neural networks (ANN) for early voltage collapse forecast in a power system. The ANN is trained using data gathered from multiple simulations, enabling the estimation of the stability margin against voltage collapse online. The L-index is employed as a simple and straightforward indicator that can be expanded to a multi-node system. The proposed technique provides a quick real-time voltage security evaluation in a power system, offering a helpful tool for prompt voltage collapse prediction. In [17], a recurrent neural network (RNN) mechanism based on voltage instability is proposed as an early predictor. The RNN is constructed using voltage phase angle data obtained from each bus in the electrical network using PMUs. The network is trained using Particle Swarm Optimization (PSO) and tested on 4-bus and 30-bus IEEE standard systems. The performance of training the RNN with the backpropagation (BP) algorithm is compared with training it using PSO. The results demonstrate that both BP and PSO training algorithms effectively forecast voltage instability. In [18], the use of instantaneous system supervision techniques to alert the power system before voltage collapse occurs is explored. Different line voltage stability indices (LVSI) are examined to determine their effectiveness in identifying the weakest lines in the power system. The IEEE 9-Bus and IEEE 14-Bus systems are used to investigate these indices and confirm their applicability. Additionally, the study introduces the use of an artificial neural network (ANN) for real-time voltage stability monitoring. The computed indices and the estimated indices using ANN are shown to be useful in predicting voltage collapse in the system.

In [19], a sliding three-dimensional convolutional neural network (3D-CNN) instantaneous continuous monitoring system (CMS) is proposed for assessing long-term voltage stability. The dynamic reactions and topological data of a power system are combined and transformed into sequential state images, which serve as input to the sliding 3D-CNN. The CMS takes into account both spatial and temporal correlation by using localized weight-shared convolution processes. The effectiveness of the proposed system is tested on the New England 10-generator-39-bus system. In [20], the author describes the use of an artificial neural network to assess the voltage stability of a power supply. The neural network maps the relationship between the operating characteristics of the power system and an energy metric that indicates how close the system is to voltage collapse. This information can be utilized by operators to initiate appropriate control actions to prevent voltage collapse. The suggested approach can be integrated into a comprehensive dynamic security analysis package as an online voltage stability assessment tool. In [21], support vector regression (SVR) is employed to forecast dynamic voltage collapse on a real power system. The Predictor of Voltage Collapse (PTSI), derived from data obtained from dynamic simulations, is used to initially anticipate dynamic voltage collapse. Simulations are conducted on a real-world 87-bus test system with load increase as the contingency. The information obtained from time-domain simulations is then fed into the SVR, which utilizes support vector regression to predict the dynamic voltage collapse indices of the power system. The selection of Kernel function type and Kernel parameter is considered to enhance training time and improve SVR accuracy. The suggested SVR approach is evaluated and compared with a multilayer perceptron neural

network (MLPNN) to confirm its effectiveness. The studies indicate that SVR performs dynamic voltage collapse forecasting tasks faster and with higher accuracy compared to MLPNN.

In [22], a novel index is proposed to evaluate voltage stability effectively. This index is developed using the network ABCD parameters and is based on an accurate model of the transmission system. One key advantage of the proposed index is its ability to forecast voltage collapse by considering the effects of the respective directions of active and reactive power flows in the transmission lines. The suggested index can accurately forecast voltage stability under various operating conditions and situations, enabling precise contingency analysis and ranking. In [23], the authors proposed an innovative approach to estimate the static voltage collapse point in power systems using a quadratic approximation. This method only requires one power flow solution and provides a more precise estimation of the collapse point. Additionally, it improves estimation accuracy for power systems under stress. The results demonstrated that it converges more quickly compared to more sophisticated methods. In [24], a novel node voltage stability index (NNVSI) is presented for forecasting static and dynamic voltage collapse occurrences. The index is based on node voltages and network admittance matrices and is applicable to an n-bus system. The NNVSI is evaluated using the IEEE New England test system and compared with other methods such as the power flow Jacobian singular value, power transfer stability index (PTSI), and modified voltage stability index (MVSI). The results show that the suggested index efficiently predicts static and dynamic voltage stability collapse points. In [25], the adaptive multi-step Levenberg-Marquardt (AMSLM) method is proposed to address the power flow issue in ill-conditioned power systems. An AMSLM continuation power flow (AMSLM-CPF) approach is presented to assess the stability of voltage, which relies on the newly suggested AMSLM power flow (PF) method. The parameters of the novel AMSLM-PF method are optimized using a fuzzy inference system (FIS). The effectiveness of the proposed AMSLM-PF and AMSLM-CPF approaches is demonstrated through comprehensive simulation results. In [26], the critical switching of capacitors is investigated to avoid voltage instability in transmission networks. Both static and dynamic methodologies are employed to analyze the issue. Static analysis is used to identify steady-state power flow solutions for different cases, including pre-disturbance steady-state, post-disturbance steady-state without VAR support, and post-disturbance steady-state with VAR support. The findings illustrate how the characteristics of aggregate load and system conditions impact critical switching time.

In [27], a novel approach is proposed that utilizes a flexible classification criterion to detect operating situations that are close to or within the range of voltage instability. Decision trees are constructed and validated using training and test data sets, and a sampling strategy is suggested to reduce computational load. Time domain simulations using PSS/E are also used to evaluate the forecasting accuracy of the decision trees, particularly in network topologies involving line outages. In [28], the analysis of voltage instability related to the AVR voltage saturation phenomenon is performed in steady-state conditions. A new approach based on the predictor-corrector technique is presented to determine the total system equilibrium of the power system model. This methodology computes Saddle Node Bifurcation (SNB) and Saddle Limit Induced Bifurcation (SLIB) points while considering the voltage limits of all generation units' AVR. The 39-bus system in New England is used as an example to demonstrate the effectiveness of the proposed approach. In [29], a novel method is proposed to calculate the probability distribution of load-space proximity to voltage instability caused by the saddle-node bifurcation point. The method also estimates the probability distribution of the time to voltage instability for a power system with unknown upcoming loading scenarios. The approach approximates the saddle-node bifurcation surface using a second-order estimation. The suggested method can be utilized in power system security assessment to quickly and effectively determine the proximity to voltage stability issues. The performance of the proposed method is evaluated using Monte Carlo simulation on a numerical example and the IEEE 9-bus test system. In [30], the authors provide a simple model of the dynamics following a saddle-node bifurcation and illustrate the loss of stability when a stable equilibrium point disappears. This finding is applicable to various types of dynamical systems with one parameter. Based on these findings, a model for voltage collapse in power networks is proposed. The model offers an explicit mechanism for the dynamics of voltage collapse. The authors demonstrate the model by constructing a straightforward power system model and simulating a voltage collapse. In [31], Ant Colony Optimization (ACO) is utilized to identify voltage collapse situations in power networks, aiming to accelerate computation for online detection and prediction in smart grid applications. Two case studies, the IEEE 118-bus system and the 9-bus system, are employed to evaluate the efficiency of the proposed detection algorithm. The approach can identify the nearest saddle-node bifurcation point in an electric power system and pinpoint the weak power system buses and the contributing factors to voltage collapse on those buses.

In [32], a new algorithm for protection against voltage collapse is proposed, which utilizes the magnitudes and angles of local phasors. The algorithm calculates a voltage collapse criterion based on the change in apparent power line flow at specific time intervals. The criterion reflects the observation that line losses increase more rapidly than apparent power delivery in the vicinity of voltage collapse. When a voltage collapse occurs, the criterion becomes zero, allowing the relay to respond promptly with the appropriate setting. The algorithm can be implemented efficiently by numerical relays and provides a straightforward and fast computation. The algorithm is evaluated using various test systems, including the New England 39-bus test system. In [33], the authors introduce the Power Transfer Stability Index as an indicator for predicting dynamic voltage collapse in power systems. The performance of this indicator is evaluated using the 9-bus and 39-bus test systems under various operating conditions. The simulation process incorporates dynamic power system models, including automatic voltage regulators, over excitation limiters, under load tap changers, and induction motors. Comparative simulation test results demonstrate that the Power Transfer Stability Index provides a comparable forecast of dynamic

voltage collapse when compared to the voltage collapse prediction index. In [34], the authors proposed the use of statistical techniques to calculate the voltage collapse proximity in a power system. The Voltage Collapse Proximity Index (VCPI) is employed to retrieve historical data for different contingencies and loading conditions, as the model-building process requires the compilation of a database. Combining this analytical approach with existing equipment in power system control centres could enable future online applications. The VCPI is a well-documented index frequently suggested as an alternative for online voltage collapse prediction. However, it requires knowledge of the electrical grid layout, which is not feasible during malfunctions such as line outages. In [35], the stability of power systems is examined using the modal analysis technique. The modal analysis approach predicts stability margins or distances to voltage collapse based on reactive power load demand. Q-V curves are also utilized to validate the results obtained through modal analysis. The analysis is conducted on two well-known power systems, the IEEE 30 Bus system and the Western System Coordinating Council (WSCC). The modal analysis technique is applied considering constant load models, voltage-dependent load models, and induction machine load models for both systems. The critical mode for each system is identified, and the participation factor is used to identify the weakest buses contributing the most to the critical mode. Q-V curves are constructed at these buses to verify the outcomes of the modal analysis method and determine the stability margin or distance to voltage collapse. In [36], the authors proposed a real-time method for estimating voltage collapse in a network using an indicator that needs to be calculated at each bus. This indicator is called the Voltage Collapse Prediction Index (VCPI). The procedure requires the network admittance matrix of the power system and voltage phasor data from the buses. The VCPI is derived at each bus using the recorded voltage phasors and the network admittance matrix, indicating the proximity of a bus to voltage collapse.

In [37], the authors proposed a voltage control technique based on Model Predictive Control (MPC) to mitigate voltage instability. The technique focuses on the capability of reactive power and the responsiveness of Under Load Tap Changers (ULTCs) to voltage drop following contingencies. By utilizing reactive power injection and tap changing, the suggested control scheme aims to prevent voltage collapse. The effectiveness of the proposed technique is demonstrated on a 4-bus power system, showing its ability to prevent voltage collapse. In [38], the authors introduce two new approaches for determining the critical point in power systems. One approach combines the fundamental methodology with a correctness method based on Continuation Power Flow (CPF). This approach improves calculation speed by avoiding the repetitive analysis of the same topology and bus types. The other approach is a direct method that leverages a fresh perspective on power systems and the fundamental physical principles of voltage collapse and critical points. The CPF is primarily considered in AC systems, while the similar CPF in DC systems is examined for comparison. Numerical verification confirms that the proposed methods reduce the computational load of the CPF method in DC systems. In [39], the authors proposed a method called relaxed decoupled direct calculation (RDDC) for locating voltage collapse points (VCPs). The direct computation of VCPs using a Newton-Raphson type method faces sensitivity issues with initial values. To address this, the RDDC method integrates with a boundary tracking method that utilizes data from neighbouring VCPs. The findings demonstrate that the RDDC method can accurately compute VCPs in less time compared to continuation power flow. When RDDC is combined with boundary tracking, the static voltage stability area boundary can be determined with high accuracy, leading to improved computational performance for various test systems ranging from nine buses to ten thousand buses. In [40], an improved method to prevent voltage collapse is proposed, which relies on repeated voltage- and current-phasor measurements to assess voltage stability at a bus. The voltage-collapse criterion is computed based on the change in apparent-power bus injection over time. The method observes that in the vicinity of voltage collapse, no more apparent power can be transferred to the affected bus. The one-step method needs to be checked only once, regardless of whether the lines are generating or absorbing reactive power. The algorithm is extensively tested on multiple test systems, including a static IEEE 30-bus system and a dynamic Belgian-French 32-bus system with comprehensive dynamic models of power system elements relevant to voltage instability analysis. The results highlight the advantages of the proposed approach, which is straightforward, computationally efficient, and suitable for implementation in a numerical relay. In [41], an integrated method is proposed to forecast voltage stability margin (VSM) quickly for static voltage stability assessment (VSA) in power systems. The method combines correlation detection (CD) and random bits forest (RBF). A feature selection framework based on CD methods is developed to select representative features closely related to VSM and with less duplication. The RBF-based forecasting model is trained using the selected feature set and associated VSM. Once real-time operating data is obtained, the trained model can rapidly generate the desired output.

In [42], the authors proposed a data-driven technique for gaining insight into voltage magnitude fluctuations using synchronous phasor measurement unit (PMU) data to prevent voltage collapse. The strategy is based on the moment-based spectrum estimation technique and introduces a new indicator called the spectrum estimation-based stability indicator (SESI), which is based on random matrix theory. The SESI, acting as an inverse Jacobian related indicator, enables improved static voltage stability assessment in power systems with a large number of measurement variables. The effectiveness of the proposed strategy is demonstrated through case studies involving the IEEE 118-bus system, the IEEE 300-bus system, and a Polish 2383-bus system. In [43], a line voltage stability index (LVSI) is presented to evaluate the stress condition and voltage stability state of lines in a power system. The index calculates the stability margin in megavolt amps (MVA). The IEEE 30-bus and IEEE 118-bus test systems are used to assess the efficacy of the proposed index, particularly its ability to accurately estimate the MVA margin under various loading situations. The derived MVA margin using the index can be utilized in congestion management of power systems. In [44], the states of a power system are

estimated using phasor measurement data from a subset of buses. A voltage stability index is determined based on the proportion of change in load power to the change in voltage magnitude, indicating the system's vulnerability to instability caused by topology or load changes. As the suggested index approaches 1, the system approaches the voltage breakdown point, while lower values indicate system stability. Load margin evaluation is conducted for stressed buses using a least squares method when the system is under voltage stress. The approach is tested on the 233-bus North Eastern Indian grid and the 39-bus New England test system with varying loads and topology, demonstrating the accuracy of the stability index calculation and load margin evaluation. In [45], the authors proposed a data-driven method for evaluating long-term voltage stability based on variational autoencoders (VAE) using PMU monitoring data. This technique utilizes unsupervised data mining and probabilistic learning to extract representative features. The method standardizes latent features in an anticipated stochastic distribution, which is different from conventional feature extraction techniques. A statistical indicator sampling latent properties after variance decline is suggested for evaluating long-term voltage stability. The method is tested on simulated power systems with various load-increasing models, demonstrating its accuracy and efficacy in determining voltage collapse points. In [46], a novel sensitivity method is developed for selecting the best control variables to reduce voltage instability in power systems. The method performs a sensitivity analysis on a voltage stability index called Thevenin-Based Voltage Stability Margin (TVSM), which is based on the coupled single-port circuit concept. The sensitivity approach calculates the changes in nodal voltages (magnitudes and angles) with respect to preventive controls. In [47], an index is proposed to assess the voltage stability condition of a power system under bus loading stress. The index is obtained from the sensitivity analysis of the maximum loadability problem based on an optimization model. By considering the difference between the maximum power transfer point and maximum loadability point, taking into account voltage-dependent loads such as ZIP and exponential models, the proposed index provides a reliable indication of voltage stability. Validation tests on two-bus and IEEE 30-bus test systems demonstrate the effectiveness of the proposed strategy.

3. MATHEMATICAL FORMULATIONS

This section presents the mathematical formulations for the existing voltage instability prediction methods including L-index-based approach.

3.1 L-Index-Based Prediction Method

The line model, which can be thought of as the most basic power system configuration and which can also be examined analytically, is the starting point for this analysis. Figure 1 shows the node 1 supplying the load which can also be called the load node or consumer node and node 2 characterized by the generator node which could be represented by a PV node or slack node. The power system is a linear transmission system that can be presented in a matrix form as expressed below, Kessel (1986);

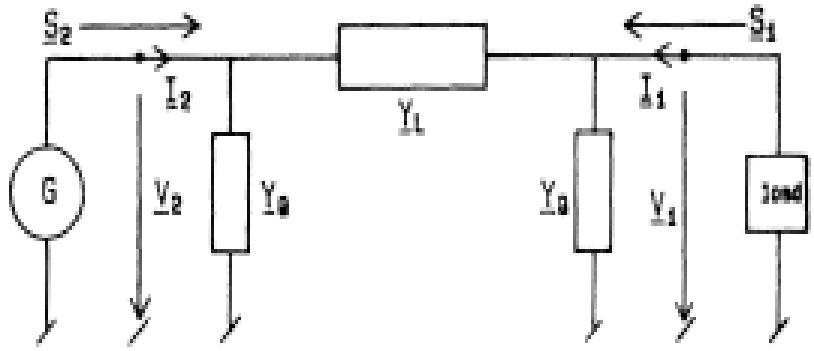

Figure 1: Line model showing the generator G; the nodal voltagesV_1, V_2; nodal currents I_1, I_2; and complex powers S_1, S_2

$$Y_{11} \times V_1 + Y_{12} \times V_2 = \left(\frac{S_1}{V_1} \right)^* \tag{1}$$

where Y_{11}, Y_{12}, Y_{21} and Y_{22} are the elements of the system admittance matrix $[Y]$.
The complex power at bus 1is

$$S_1 = V_1 \times I_1^* \tag{2}$$

From Equation (1),

$$V_1^* \times V_1 + V_1^* \times \frac{Y_{12}}{Y_{11}} \times V_2 = \frac{S_1^*}{Y_{11}} \tag{3}$$

Let

$$\frac{Y_{12}}{Y_{11}} \times V_2 = V_0 \tag{4}$$

Using Equation (4) in Equation (3) results in

$$V_1^* \times V_1 + V_1^* \times V_0 = \frac{S_1^*}{Y_{11}} = a_1 + jb_1 \tag{5}$$

where a_1 represents the real component of Equation (5) and b_1 represents the imaginary component
That is

$$a_1 = V_0 \times V_1 \cos\delta + V_1^2 \tag{6}$$

$$b_1 = V_0 \times V_1 \sin\delta \tag{7}$$

From Figure 1, we can write

$$\frac{Y_{12}}{Y_{11}} = \frac{Y_L}{Y_L + Y_Q} \tag{8}$$

where
Y_L is the series admittance of the network π -model
Y_Q is the shunt admittance of the network π -model
Expansion of equation (5) gives

$$a_1 + jb_1 = V_1^2 + V_0 \times V_1 \cos\left(\delta_0 - \delta_1\right) + jV_0 \times V_1 \sin\left(\delta_0 - \delta_1\right) \tag{9}$$

From (7), $\cos\left(\delta_0 - \delta_1\right) = \dfrac{a_1 - V_1^2}{V_0 \times V_1}$ (10)

$$\sin\left(\delta_0 - \delta_1\right) = \frac{b_1}{V_0 \times V_1} \tag{11}$$

Squaring Equations (10) and (11) gives

$$V_0^2 \times V_1^2 = \left(a_1 - V_1^2\right)^2 + b_1^2 = a_1^2 - 2a_1V_1^2 + V_1^4 + b_1^2 \tag{12}$$

Manipulation of Equation (12) gives

$$V_1 = \sqrt{\left(\frac{V_0^2}{2} + a_1\right) + \sqrt{\left(\frac{V_0^4}{4} + a_1V_0^2 - b_1^2\right)}} \tag{13}$$

Or $$V_1 = \sqrt{\frac{S_1}{Y_{11}}\left(r \pm \sqrt{\left(r^2 - 1\right)}\right)} \tag{14}$$

where

$$r = \frac{V_0^2 \times \mathrm{Y}_{11}}{2 \times S_1} + \cos\left(\Phi_{S_1} + \Phi_{Y_{11}}\right) \tag{15}$$

and Φ represents an angle of a complex number, Substituting Equation (4) into Equation (3) gives

$$\left|S_1 - Y_{11} \times V_1^2\right| = V_0 - V_1 \times Y_{11} \tag{16}$$

The geometric interpretation of Equation (14) is that all states with amplitudes V_1 that are constant lie on circles on the complex S_1-plane with the radius being determined by $Y_{11}.V_0.V_1$ and the centre by $Y_{11}.V_1$ This scenario for a particular numerical example of a line is shown in Figure 2. Plotted are circles of constant voltage for V_1= 0.8, 1.0 and 1.2 pu. (+) refers to the solution with the feasibly larger amplitude V_1, and (-) refers to the solution with a smaller amplitude.

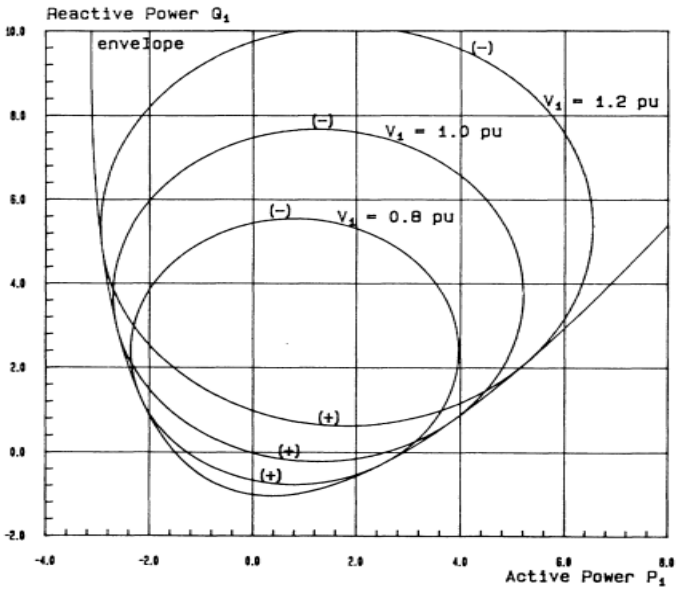

Figure 2: Circles of constant voltage amplitude V_1

A collection of circles is created when V_1 is changed inside the acceptable area, which is determined by S_1, whose union creates the feasible state space in $D = \{V_1 \mid 0 \le V_1 < \infty\}$. The desired stability limit of the current two-node system is the boundary curve of this region, or the envelope of all these circles. No physical significant solutions are feasible outside of the curve.

The Jacobian matrix of the simple 2-bus system can be written as

$$\text{Jac} = \begin{bmatrix} \dfrac{\partial f}{\partial V_1} & \dfrac{\partial f}{\partial \delta} \\ \dfrac{\partial g}{\partial V_1} & \dfrac{\partial g}{\partial \delta} \end{bmatrix} \tag{16}$$

where $f(V_1, \delta)$ and $g(V_1, \delta)$ are defined in Equations (6) and (7) respectively.

$$\text{Jac} = \begin{bmatrix} 2V_1 + V_0 \cos\delta & -V_1 V_0 \\ V_0 \sin\delta & V_1 V_0 \cos\delta \end{bmatrix} \tag{17}$$

It can be easily shown that when the voltage collapse occurs at bus 1, using Equation (11), we can write

$$\sqrt{\left(\frac{V_0^4}{4} + a_1 V_0^2 - b_1^2\right)} = 0 \tag{18}$$

Also, the determinant of equation (17) equals zero at the collapse point. Therefore,

$$\det(\text{Jac}) = 2V_1^2 V_0 \cos\delta + V_0^2 V_1 = 0 \tag{19}$$

From Equation (19),

$$\frac{V_1 \cos\delta}{V_0} = \Re\left\{\frac{V_1}{V_0}\right\} = \frac{-1}{2} \tag{20}$$

By dividing Equation (3) by $V_1^2 Y_{11}$, we have

$$\left|1+\frac{V_0}{V_1}\right| = \left|\frac{S_1}{Y_{11}\times V_1^2}\right| = 1 \tag{21}$$

With the use of this relationship, an indicator for L for evaluating voltage stability may be defined. For the workable solution with the huge voltage amplitude V_1, its range is

$$R = \{\mathrm{L} \mid 0 \le L < 1\} \tag{22}$$

Therefore,

$$L = \left|1+\frac{V_0}{V_1}\right| = \left|\frac{S_1}{Y_{11}\times V_1^2}\right| = r + \sqrt{r^2 - 1} \tag{23}$$

And

$$S_1 = \frac{Y_{11}\times V_0^2}{L + \frac{1}{L} - 2\times\cos Y_{11}\left(\Phi_{S_1} + \Phi_{Y_{11}}\right)} \tag{23}$$

Figure 3 shows the geometric relationship when the values for the line curves of $L =$ 0.2, 0.4, 0.6, 0.8, 1.0 are plotted.

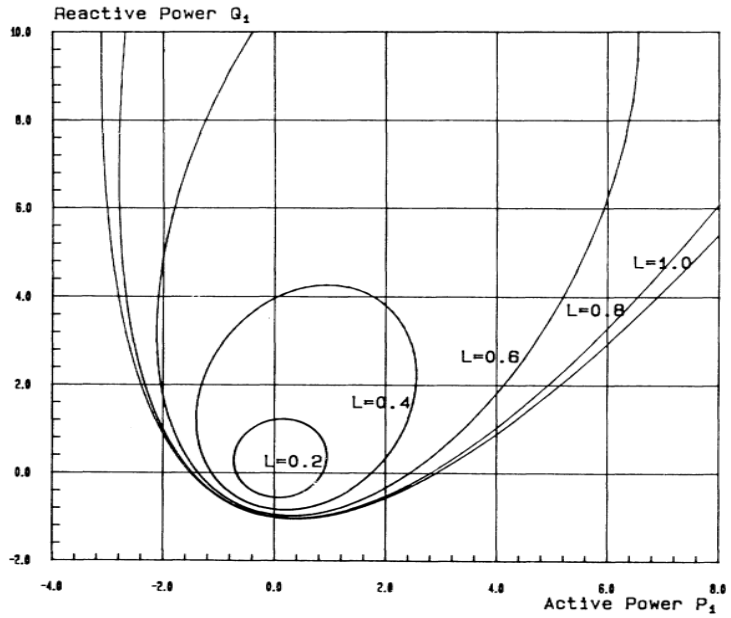

Figure 3: Indicator L in the complex $\underline{S_1}$ plane

Since the transmission system can be represented using a hybrid (H) matrix

$$\begin{vmatrix} V^L \\ I^G \end{vmatrix} = |H| \times \begin{vmatrix} I^L \\ V^G \end{vmatrix} = \begin{vmatrix} \|Z^{LL}\| & \|F^{LG}\| \\ \|K^{GL}\| & \|Y^{GG}\| \end{vmatrix} \times \begin{vmatrix} I^L \\ V^G \end{vmatrix} \tag{24}$$

V^L, I^L are the voltage and current vectors at consumer nodes

V^G, I^G are the voltage and current vectors at generator nodes

Z^{LL}, F^{LG}, K^{GL}, Y^{GG} are the submatrices of H-matrix

For any consumer nodes $j, J \in \alpha_{L.}$

$$V_{-j} = \sum_{i\varepsilon\alpha_L} Z_{-ji} \times I_{-i} + \sum_{i\varepsilon\alpha_L} F_{-ji} \times V_i \tag{25}$$

Alternatively,

$$V_j^2 + V_{-0j} \times V_j^* = \frac{S_{-j}^{+*}}{Y_{-jj}^+} \tag{26}$$

From equation (23), a local indicator $\left(L_j\right)$ that is similar to the line model can be developed for each node j

$$L_j = \left|1 + \frac{V_{-0j}}{V_{-j}}\right| = \left|\frac{S_{-j}^+}{Y_{-11}^{+*} \times V_{-j}^2}\right| \tag{27}$$

where

$$V_{-0j} = -\sum_{i\varepsilon\alpha_G} F_{-ji} \times V_{-i} \tag{28}$$

$$Y_{-jj}^+ = \frac{1}{Z_{-jj}} \tag{29}$$

$$S_{-j}^+ = S_{-j} + S_{-j}^{corr} \tag{30}$$

$$S_{-j}^{corr} = \left(\sum_{i\neq j} i\varepsilon\alpha_L \frac{Z_{-ji}^*}{Z_{-jj}^*} \times \frac{S_{-i}}{V_{-i}} \right) \times V_{-j} \tag{31}$$

α_L = Constant of nodes set

α_G = generator nodes set

For all nodes j, the condition for the indicator L, which describes the entire system stability is

$$L = \underset{j\varepsilon\alpha_L}{MAX} \left\{L_j\right\} \tag{32}$$

$$L = \underset{J\varepsilon\alpha_L}{MAX} \left|1 - \frac{\sum_{i\varepsilon\alpha_G} F_{-ji} \times V_{-i}}{V_{-j}}\right| \tag{33}$$

Hence the major outcome of the theory discussed for stability to occur is

$$L < 1 \tag{34}$$

3.2 Existing Voltage Collapse Prediction Methods

i. Voltage Stability Index (L_P): The line stability index proposed in [48] has a similar mathematical formulation to earlier line VSIs and basically defined as

$$L_p = \frac{4RP_r}{[V_s \cos(\theta - \delta)]^2} \leq 1 \tag{35}$$

The L_P defined in Equation (35) determines the condition of the transmission line and indicates instability limits. If the calculated value of L_p is more significant to the unity, the system approaches instability. The voltage collapses when the system exceeds the critical limits.

ii. Fast Voltage Stability Index (FVSI): The Fast Voltage Stability Index (FVSI) [48] primarily considered the current through the line and then absolute roots of a receiving-end voltage is determined. This is usually formulated as

$$FVSI = \frac{4Z^2 Q_r}{V_s^2 X} \tag{36}$$

The line is in-transit to the instability limit if the FVSI value is adjacent to 1. With further increases in a stability index value, that line may encounter an unexpected voltage drop accompanying system collapse.

iii. Voltage Stability Load Bus Index (VSLBI): Voltage Stability Load Bus Index (VSLBI) evaluates the voltage stability by employing PMU applications [49]. Considering the maximum power condition, this stability index is subject to a voltage-drop ΔVr over the transmission impedance Zr that is equivalent to load bus voltage Vr:

$$\Delta V_r = V_r \tag{37}$$

Accordingly, to approach the voltage collapse exposure during the constant power loads, the Voltage Stability Load Bus Index (VLSBI) can be represented by

$$\text{VSLBI} = \frac{V_r}{\Delta V} \tag{38}$$

If the obtained value of the VSLBI is more significant than the unity, then the system is considered stable; if the VSLBI is less than 1, then the system is unstable, and the system may collapse.

4. RESULTS AND DISCUSSION

This section presents the simulation results as well as the discussion of the results obtained using the two case studies of the standard IEEE 30-bus system and the Nigerian 28-bus 330kVgrid network.

4.1 Case Study 1: Results of Power Flow on IEEE 30-Bus System

In this section, we present the results of the MATLAB simulations conducted, on the IEEE 30-bus and the Nigerian 330-kV system, to identify the weakest bus using the L-index methodology. The load flow analysis was initially performed on the IEEE 30-bus system to determine the voltage magnitudes at each bus and the line flow and losses in the network. The results are presented in Table 1 and Table 2.

Table 1: Bus voltage magnitudes in the original IEEE 30-bus system

BUS NO	V (P.U)	BUS NO	V (P.U)	BUS NO	V (P.U)	BUS NO	V (P.U)
1	1.06	9	1.05	17	1.04	25	1.02
2	1.04	10	1.04	18	1.03	26	1.00
3	1.02	11	1.08	19	1.03	27	1.03
4	1.01	12	1.06	20	1.03	28	1.01
5	1.01	13	1.07	21	1.03	29	1.01
6	1.01	14	1.04	22	1.03	30	0.99
7	1.00	15	1.04	23	1.03		
8	1.01	16	1.04	24	1.02		

From Table 1, it can be observed that all thirty buses have voltage magnitudes within the statutory voltage limit of 0.95 - 1.1 per unit (p.u). The lowest voltage magnitude is recorded at bus 30, which is 99% of the nominal voltage.

Table 2: Line results for the 30-Bus IEEE network

FROM	TO	P (MW)	Q (Mvar)	P (MW)	Q (Mvar)	Ploss (MW)	Qloss (Mvar)
1	2	177.78	-22.15	-172.31	32.67	5.46	10.52
1	3	83.22	5.13	-80.41	1.96	2.81	7.09
2	4	45.71	2.70	-44.61	-3.22	1.11	-0.52
……							
28	27	18.18	5.47	-18.18	-4.16	0.00	1.31
28	8	0.58	-2.00	-0.58	-2.37	0.00	-4.37
29	30	3.70	0.61	-3.67	-0.54	0.03	0.06
TOTAL LOSS						**17.5985**	**22.2444**

i. L-index analysis results

To identify the weakest bus in the IEEE 30-bus system, the L-index analysis was performed by gradually increasing the active load on the system from 100% to 320% in 10% increments. The bus voltage magnitudes and L-index values were recorded at each load level as shown in Tables 3 and 4.

Table 3: Bus Voltage results for the 30-Bus IEEE network at 320% loadability of active load power

BUS NO	V (P.U)	BUS NO	V (P.U)	BUS NO	V (P.U)	BUS NO	V (P.U)
1	1.06	9	0.93	17	0.87	25	0.77
2	0.99	10	0.89	18	0.83	26	0.72
3	0.84	11	1.08	19	0.82	27	0.78
4	0.83	12	0.91	20	0.84	28	0.87
5	0.96	13	1.02	21	0.85	29	0.69
6	0.88	14	0.87	22	0.85	30	0.63
7	0.89	15	0.85	23	0.82		
8	0.96	16	0.88	24	0.80		

Table 4: Load bus L-Index results for the 30-Bus IEEE network at 320% loading of active load

LOAD BUS	L-Index	LOAD BUS	L-Index	LOAD BUS	L-Index	LOAD BUS	L-Index
3	0.068	14	0.307	21	0.87	28	0.094
4	0.078	15	0.335	22	0.388	29	0.740
6	0.066	16	0.286	23	0.416	30	0.950
7	0.086	17	0.337	24	0.474		
9	0.165	18	0.420	25	0.517		
10	0.320	19	0.446	26	0.643		
12	0.202	20	0.419	27	0.485		

Table 3 shows the trend of bus voltage magnitudes as the system is subjected to increasing load levels. It can be observed that bus voltages decrease as the load increases, which is a common characteristic in power systems. Table 4 shows the behaviour of the L-index values for each bus as the active power load increases from 100% to 320%. A lower L-index value indicates a more stable bus, while a higher L-index value indicates a weaker bus and a closer proximity to voltage collapse. From Table 4, it is evident that bus 30 has the highest L-index curve, followed by buses 29 and 26. This implies that bus 30 is the weakest bus in the system, followed by bus 29 and bus 26, as they have the highest L-index values. The L-index values for bus 30, 29, and 26 at 320% loading are 0.95, 0.74, and 0.643, respectively.

ii. Result after applying STATCOM device

To assess the effectiveness of using STATCOM devices to enhance voltage stability and mitigate the risk of voltage collapse, 5 MVar STATCOM devices were incorporated at buses 26, 29, and 30 while ensuring that the voltage limits (0.95 - 1.1 p.u) were not exceeded. The load flow and L-index analysis were performed again with the STATCOM devices.

Table 5: Voltage magnitude at buses 26, 29, and 30 before STATCOM

LOAD BUS	26	29	30
L-Index	0.068	0.740	0.950

Table 6: Bus results for the 30-Bus IEEE network with STATCOM at buses 26, 29 and 30

BUS NO	V (P.U)	BUS NO	V (P.U)	BUS NO	V (P.U)	BUS NO	V (P.U)
1	1.06	9	1.05	17	1.04	25	1.06
2	1.04	10	1.05	18	1.03	26	1.06
3	1.02	11	1.08	19	1.03	27	1.07
4	1.01	12	1.06	20	1.04	28	1.02
5	1.01	13	1.07	21	1.04	29	1.07
6	1.01	14	1.05	22	1.04	30	1.0608
7	1.00	15	1.04	23	1.04		
8	1.01	16	1.05	24	1.04		

Table 7: Line flow and losses with STATCOM devices at buses 26, 29, and 30

FROM	TO	P (MW)	Q (Mvar)	P (MW)	Q (Mvar)	Ploss (MW)	Qloss (Mvar)
1	2	177.717	-22.134	-172.258	32.646	5.460	10.513
1	3	83.265	4.373	-80.458	2.701	2.807	7.074
2	5	82.921	1.709	-79.931	6.448	2.990	8.157
……..							
28	8	0.348	0.807	-0.342	-5.181	0.006	-4.375
12	13	0.000	-7.963	0.000	8.042	0.000	0.079
11	9	0.000	14.302	0.000	-13.939	0.000	0.363
TOTAL LOSS						**17.5826**	**21.7165**

Table 8: Bus voltage results for the 30-Bus IEEE network at 350% loading of the active power after applying STATCOM at buses 26, 29 and 30

BUS NO	V (P.U)	BUS NO	V (P.U)	BUS NO	V (P.U)	BUS NO	V (P.U)	BUS NO	V (P.U)
1	1.060	7	0.864	13	1.021	19	0.770	25	0.755
2	0.993	8	0.960	14	0.821	20	0.784	26	0.722
3	0.763	9	0.894	15	0.805	21	0.806	27	0.766
4	0.773	10	0.843	16	0.840	22	0.806	28	0.839
5	0.960	11	1.082	17	0.829	23	0.775	29	0.694
6	0.840	12	0.872	18	0.775	24	0.761	30	0.637

Table 9: L-Index results for the 30-bus IEEE network at 350% loading of the active load power after applying STATCOM at buses 26, 29 and 30

LOAD BUS	L-Index	LOAD BUS	L-Index	LOAD BUS	L-Index	LOAD BUS	L-Index
3	0.085	12	0.243	19	0.546	25	0.602
4	0.096	14	0.372	20	0.512	26	0.735
6	0.078	15	0.407	21	0.469	27	0.557
7	0.100	16	0.345	22	0.468	28	0.110
9	0.196	17	0.407	23	0.504	29	0.826
10	0.385	18	0.514	24	0.570	30	1.048

Table 6 shows the bus results of the IEEE 30-bus power system after the integration of STATCOM at buses 26, 29, and 30. It can be observed that the voltage profile has improved, and there is a slight reduction in active power loss from 17.5985 MW to 17.5826 MW and reactive power loss from 22.2444 MVAr to 21.7165 MVAr as indicated in Table 7.

The results presented in Table 8 shows that bus 30, followed by buses 29 and 26, have the lowest bus voltage magnitude trend as the active power load increases by 10% from 100% to 350% however, the voltage profile is improved compared to the case without STATCOM devices. The voltage magnitudes for these buses at 350% loadability are 0.637, 0.694, and 0.722, respectively.

Table 9 presents the Load Bus L-Index results versus loadability for the 30-Bus IEEE Network after incorporating the STATCOM devices. It shows the L-index values for each bus as the active power load increases by 10% from 100% to 350%. Although the values of buses 30, 29, and 26 still have the highest L-index values, indicating that they are the weakest buses, their L-index values have improved compared to Table 4 where STATCOM devices were not applied.

4.2 Case Study 2: Results of Power Flow on Nigerian 28-Bus, 330kV System

In this section, we present the results of the MATLAB simulations conducted on the Nigerian 28-bus 330kV system to identify the weakest bus using the L-index methodology. The load flow analysis was initially performed on the Nigerian 28-bus 330kV system to determine the voltage magnitudes at each bus and the line flow and losses in the network. The results are presented in Table 10 and Table 11.

It can be seen from the simulation results presented in Table 10 that only bus 16 is out of the voltage limit range (0.95 - 1.05 p.u), while Table 11 shows the line flow and losses in the Nigeria 28-bus system, with a total active power loss of 93.84 MW and a total reactive power loss of -727.23 MVAr.

Table 10: Bus voltage magnitudes in the original Nigerian 28-bus 330kV system

BUS NO	V (P.U)	BUS NO	V (P.U)	BUS NO	V (P.U)	BUS NO	V (P.U)	BUS NO	V (P.U)
1	1.05	7	1.05	13	0.95	19	1.00	25	1.01
2	1.05	8	1.03	14	0.97	20	1.01	26	1.03
3	1.04	9	0.97	15	1.03	21	1.05	27	1.05
4	1.01	10	1.01	16	0.90	22	0.96	28	1.05
5	1.02	11	1.05	17	1.05	23	1.05		
6	1.04	12	1.03	18	1.05	24	1.05		

Table 11: Line results for the 28-bus system

FROM	TO	P(MW)	Q(Mvar)	P(MW)	Q (Mvar)	Ploss (MW)	Qloss (Mvar)
1	3	137.36	100.82	-137.20	-102.90	0.16	-2.08
1	3	137.36	100.82	-137.20	-102.90	0.16	-2.08
2	8	330.17	32.64	-325.84	-23.43	4.33	9.22
……							
27	25	375.00	29.34	-364.74	5.86	10.26	35.20
28	5	375.00	223.81	-372.20	-213.13	2.80	10.68
28	5	375.00	223.81	-372.20	-213.13	2.80	10.68
Total Loss						**93.84**	**-727.23**

i. L-index analysis results

To identify the weakest bus in the Nigerian 28-bus 330kV system, the L-index analysis was performed by gradually increasing the active load on the system from 100% to 190% in 10% increments. The bus voltage magnitudes and L-index values were recorded at each load level as presented in Tables 12 and 13.

Table 12: Bus voltage results for the Nigerian 28-bus 330kV system at 190% loading of active load power

BUS NO	V (P.U)	BUS NO	V (P.U)	BUS NO	V (P.U)	BUS NO	V (P.U)	BUS NO	V (P.U)
1	1.05	7	1.04	13	0.78	19	0.95	25	0.99
2	1.05	8	0.95	14	0.81	20	0.97	26	1.01
3	1.04	9	0.82	15	1.02	21	1.05	27	1.05
4	0.91	10	0.93	16	0.78	22	0.90	28	1.00
5	0.92	11	1.05	17	1.04	23	1.04		
6	0.96	12	1.01	18	1.05	24	1.03		

Table 13: Load bus L-Index results for the Nigerian 28-bus 330kv system at 190% loading of active load

LOAD BUS	L-Index	LOAD BUS	L-Index	LOAD BUS	L-Index	LOAD BUS	L-Index
3	0.011	8	0.083	14	0.335	20	0.151
4	0.117	9	0.277	15	0.106	22	0.357
5	0.095	10	0.122	16	0.685	25	0.124
6	0.092	12	0.057	17	0.006	26	0.080
7	0.011	13	0.431	19	0.226		

Table 12 shows the bus voltage results versus loadability for the Nigeria 28-bus network as the active power load continuously increases by 10%. It can be observed that the base case result stops converging at a loadability of approximately 190% of the original active power load at all buses. Table 13 presents the load bus L-Index results versus loadability for the Nigeria 28-bus network as the active power load continuously increases by 10%. The L-Index values indicate that bus 16 has the highest L-Index, followed by bus 13 and bus 22, at a loadability of 190%. This implies that bus 16 is the weakest bus in the system, followed by bus 13 and then bus 22.

ii. Results after applying STATCOM device

To assess the effectiveness of using STATCOM devices to enhance voltage stability and mitigate the risk of voltage collapse, 5 MVar STATCOM devices were incorporated at buses 13 and 16 while ensuring that the voltage limits (0.95 - 1.05 p.u) were not exceeded. The load flow and L-index analysis were performed again with the STATCOM devices.

After incorporating STATCOM devices at Bus 13 and 16 in the Nigeria 28-bus power system, the bus results and line results are presented in Tables 15 and 16, respectively. The bus results indicate improved voltage profiles, and the active power loss is reduced from 93.84 MW to 88.10 MW, while the reactive power loss is reduced from -727.23 MVAr to -802.20 MVAr. The results presented in Table 17 show the bus voltage results for the Nigeria 28-bus network after applying STATCOM devices at Bus 13 and 16. It shows that the voltage profiles have improved compared to the base case.

Table 14: Voltage magnitude at buses 13 and 16 before STATCOM

LOAD BUS	16	13
L-Index	0.685	0.431

Table 15: Bus results for the Nigerian 28-bus 330kV system with STATCOM at buses 13 and 16

BUS NO	V (P.U)	BUS NO	V (P.U)	BUS NO	V (P.U)	BUS NO	V (P.U)	BUS NO	V (P.U)
1	1.05	7	1.05	13	1.05	19	1.03	25	1.03
2	1.05	8	1.04	14	1.03	20	1.02	26	1.03
3	1.04	9	0.97	15	1.03	21	1.05	27	1.05
4	1.01	10	1.02	16	1.04	22	0.97	28	1.05
5	1.02	11	1.05	17	1.05	23	1.05		
6	1.04	12	1.04	18	1.05	24	1.05		

Table 16: Line flow and losses with STATCOM devices at buses 13 and 16

FROM	TO	P(MW)	Q(Mvar)	P(MW)	Q(Mvar)	Ploss (MW)	Qloss (Mvar)
1	3	137.36	100.82	-137.20	-102.90	0.16	-2.08
1	3	137.36	100.82	-137.20	-102.90	0.16	-2.08
2	8	330.96	9.01	-326.67	-0.24	4.29	8.77
……..							
27	25	375.00	2.64	-364.88	30.88	10.12	33.52
28	5	375.00	218.31	-372.23	-207.90	2.77	10.41
28	5	375.00	218.31	-372.23	-207.90	2.77	10.41
Total Loss						**88.10**	**-802.20**

Table 18 presents the load bus L-Index results for the Nigeria 28-bus network after incorporating STATCOM at buses 13 and 16. It can be observed that the L-Index results stop converging at a loadability of approximately 200% of the original active power load at all buses. The L-Index values show that bus 16, followed by bus 22, bus 9 and bus 14 now have the highest L-Index values, indicating relatively weaker buses. On the other hand, bus 9 has the smallest bus voltage magnitudes compared to other buses as the loadability increases. It is worth noting that the curves of bus 16, bus 22, bus 9 and bus 14 have improved compared where STATCOM devices were not applied.

Overall, the incorporation of STATCOM devices at buses 13 and 16 in the Nigeria 28-bus system has resulted in improved voltage profiles, reduced active and reactive power losses, and enhanced voltage stability. The L-Index values and bus voltage magnitudes provide valuable information about the vulnerability of specific buses and guide the implementation of corrective measures to mitigate voltage collapse risks.

Table 17: Bus voltage result for the Nigerian 28-bus network at 200% loading of the active load power after applying STATCOM to buses 13 and 16

BUS NO	V (P.U)	BUS NO	V (P.U)	BUS NO	V (P.U)	BUS NO	V (P.U)	BUS NO	V (P.U)
1	1.05	**7**	1.03	**13**	0.86	**19**	0.98	**25**	1.00
2	1.05	**8**	0.93	**14**	0.85	**20**	0.97	**26**	1.00
3	1.04	**9**	0.74	**15**	1.02	**21**	1.05	**27**	1.05
4	0.87	**10**	0.88	**16**	0.94	**22**	0.89	**28**	1.00
5	0.88	**11**	1.05	**17**	1.03	**23**	1.03		
6	0.93	**12**	1.02	**18**	1.04	**24**	1.02		

Table 18: Load bus L-index results for the Nigeria 28-bus network at 200% loading of the active load power after applying STATCOM to buses 13 and 16

LOAD BUS	L-Index	LOAD BUS	L-Index	LOAD BUS	L-Index	LOAD BUS	L-Index
3	0.012	8	0.090	14	0.303	20	0.156
4	0.133	9	0.351	15	0.111	22	0.375
5	0.107	10	0.143	16	0.490	25	0.117
6	0.100	12	0.056	17	0.007	26	0.086
7	0.012	13	0.367	19	0.206		

5. CONCLUSION

In this study, the L-Index methodology was applied to assess voltage stability and identify the weakest buses in the IEEE 30-bus and Nigeria 28-bus power systems. The L-Index methodology effectively identified the weakest buses in both systems by correlating L-Index values with voltage magnitudes. Consistently, buses with the lowest voltage magnitudes and highest L-Index values were recognized as the weakest. Incorporating STATCOM devices at the weakest buses improved voltage profiles and reduced power losses while preserving the weak bus identification, affirming the L-Index's accuracy in predicting vulnerable buses. This study underscores the significance of voltage stability analysis and the effectiveness of the L-Index methodology in recognizing and addressing voltage instability problems. Identifying weak buses enables operators and planners to prioritize measures like installing reactive power compensation devices to boost voltage stability and prevent collapses. The utilization of the L-Index as a predictive tool has proven to be effective in assessing the proximity to voltage collapse and identifying potential instability risks in power systems. Additionally, the development of techniques for voltage stability enhancement based on the L-Index has shown promise in mitigating voltage instability and improving grid resilience.

Building upon the findings of this research, the following recommendations are made for further studies:

i. Integration with Control Strategies: Explore the integration of L-Index-based techniques with advanced control strategies, such as adaptive voltage control, reactive power optimization, and load shedding schemes. By combining predictive analysis with proactive control actions, voltage stability can be enhanced more effectively, especially in dynamic and rapidly changing operating conditions.
ii. Real-Time Implementation: Investigate the feasibility of implementing L-Index-based techniques in real-time monitoring and control systems for electrical power systems. Develop algorithms and software tools that can continuously assess voltage stability and provide timely recommendations for corrective actions to prevent voltage collapse and ensure grid reliability.
iii. Resilience Assessment: Expand the scope of research to include resilience assessment and enhancement strategies in addition to voltage stability. Consider the interdependencies between voltage stability, transient stability, and resilience to extreme events, such as natural disasters or cyber-attacks, and develop comprehensive approaches for enhancing overall grid resilience.

REFERENCES

[1] Alayande, A. S., Jimoh, A. A. G., & Yusuff, A. A., (2020), Identification of Critical Elements in Interconnected Power Networks, *Iranian Journal of Science and Technology - Transactions of Electrical Engineering*, *44*(1), 197–211.

https://doi.org/10.1007/s40998-019-00235-1
[2] Alayande, A., A.O, S., Somefun, T., Ademola, A., Awosope, C., Okoyeigbo, O., & Popoola, O., (2021), Transient Stability Enhancement of a Power System Considering Integration of FACT Controllers Through Network Structural Characteristics Theory, *Advances in Science, Technology and Engineering Systems Journal*, *6*(1), 968–981. https://doi.org/10.25046/aj0601107
[3] Zohre Alipour, M. A. S. M., (2013), Structural Properties and vulnerability of Iranian 400kv Power Transmission Grid: a Complex Systems Approach, *Industrial Engineering & Management*, *2*(3), 1–7. https://doi.org/10.4172/2169-0316.1000112
[4] Abedi, A., Gaudard, L., & Romerio, F., (2018), Review of major approaches to analyze vulnerability in power system, *Reliability Engineering and System Safety*, 153–172. https://doi.org/10.1016/j.ress.2018.11.019
[5] Hailu, E. A., Nyakoe, G. N., & Muriithi, C. M., (2023), Techniques of power system static security assessment and improvement: A literature survey, *Heliyon*, *9*(3), e14524. https://doi.org/10.1016/j.heliyon.2023.e14524
[6] Asadi Majd, A., Farjah, E., Rastegar, M., & Bacha, S., (2021), Generation and transmission expansion planning for bulk renewable energy export considering transmission service cost allocation, *Electric Power Systems Research*, *196*(October 2020), 107197. https://doi.org/10.1016/j.epsr.2021.107197
[7] Power quality and stability improvement of more - electronics power systems, (2018).
[8] Velayati, M. H., Amjady, N., & Khajevandi, I., (2015), Prediction of dynamic voltage stability status based on Hopf and limit induced bifurcations using extreme learning machine, *International Journal of Electrical Power and Energy Systems*, *69*, 150–159. https://doi.org/10.1016/j.ijepes.2015.01.005
[9] Pinzón, J. D., & Colomé, D. G., (2019), Real-time multi-state classification of short-term voltage stability based on multivariate time series machine learning, *International Journal of Electrical Power and Energy Systems*, *108*, 402–414. https://doi.org/10.1016/j.ijepes.2019.01.022
[10] Malbasa, V., Zheng, C., Chen, P. C., Popovic, T., & Kezunovic, M., (2017), Voltage Stability Prediction Using Active Machine Learning, *IEEE Transactions on Smart Grid*, *8*(6), 3117–3124. https://doi.org/10.1109/TSG.2017.2693394
[11] Wokoma, B. A., Osegi, E. N., & Idachaba, A. O., (2019), Predicting Voltage Stability Indices of Nigerian 330kV 30 Bus Power Network Using an Auditory Machine Intelligence Technique, *IEEE AFRICON Conference*, *2019-Septe*. https://doi.org/10.1109/AFRICON46755.2019.9133915
[12] Krishnan, V., & McCalley, J. D., (2012), Contingency assessment under uncertainty for voltage collapse and its application in risk based contingency ranking, *International Journal of Electrical Power and Energy Systems*, *43*(1), 1025–1033. https://doi.org/10.1016/j.ijepes.2012.05.065
[13] Wang, G., Zhang, Z., Bian, Z., & Xu, Z., (2021), A short-term voltage stability online prediction method based on graph convolutional networks and long short-term memory networks, *International Journal of Electrical Power and Energy Systems*, *127*. https://doi.org/10.1016/j.ijepes.2020.106647
[14] Ghaghishpour, A., & Koochaki, A., (2020), An intelligent method for online voltage stability margin assessment using optimized ANFIS and associated rules technique, *ISA Transactions*, *102*, 91–104. https://doi.org/10.1016/j.isatra.2020.02.028
[15] Rahi, O. P., Yadav, A. K., Malik, H., Azeem, A., & Bhupesh, K., (2012), Power system voltage stability assessment through artificial neural network, *Procedia Engineering*, *30*, 53–60. https://doi.org/10.1016/j.proeng.2012.01.833
[16] Salama, M. M., Saied, E. M., Abou-Elsaad, M. M., & Ghariany, E. F., (2001), Estimating the voltage collapse proximity indicator using artificial neural network, *Energy Conversion and Management*, *42*(1), 69–79. https://doi.org/10.1016/S0196-8904(00)00023-6
[17] Ibrahim, A. M., & El-Amary, N. H., (2018), Particle Swarm Optimization trained recurrent neural network for voltage instability prediction, *Journal of Electrical Systems and Information Technology*, *5*(2), 216–228. https://doi.org/10.1016/j.jesit.2017.05.001
[18] Goh, H. H., Chua, Q. S., Lee, S. W., Kok, B. C., Goh, K. C., & Teo, K. T. K., (2015), Evaluation for Voltage Stability Indices in Power System Using Artificial Neural Network, *Procedia Engineering*, *118*, 1127–1136. https://doi.org/10.1016/j.proeng.2015.08.454
[19] Cai, H., & Hill, D. J., (2022), A real-time continuous monitoring system for long-term voltage stability with sliding 3D convolutional neural network, *International Journal of Electrical Power and Energy Systems*, *134*. https://doi.org/10.1016/j.ijepes.2021.107378
[20] Jeyasurya, B., (1994), Artificial neural networks for power system steady-state voltage instability evaluation, *Electric Power Systems Research*, *29*(2), 85–90. https://doi.org/10.1016/0378-7796(94)90065-5
[21] Nizam, M., Mohamed, A., & Hussain, A., (2010), Dynamic voltage collapse prediction in power systems using support vector regression, *Expert Systems with Applications*, *37*(5), 3730–3736. https://doi.org/10.1016/j.eswa.2009.11.052
[22] Tiwari, R., Niazi, K. R., & Gupta, V., (2012), Line collapse proximity index for prediction of voltage collapse in power systems, *International Journal of Electrical Power and Energy Systems*, *41*(1), 105–111. https://doi.org/10.1016/j.ijepes.2012.03.022
[23] Pama, A., & Radman, G., (2009), A new approach for estimating voltage collapse point based on quadratic approximation of PV-curves, *Electric Power Systems Research*, *79*(4), 653–659.

https://doi.org/10.1016/j.epsr.2008.09.018
[24] Woldu, T. A., Ziegler, C., & Wolter, M., (2020), A new method for prediction of static and dynamic voltage collapse using node parameters in large power networks, *IEEE PES Innovative Smart Grid Technologies Conference Europe*, *2020-Octob*, 344–348. https://doi.org/10.1109/ISGT-Europe47291.2020.9248887
[25] Pourbagher, R., Derakhshandeh, S. Y., & Hamedani Golshan, M. E., (2022), An adaptive multi-step Levenberg-Marquardt continuation power flow method for voltage stability assessment in the Ill-conditioned power systems, *International Journal of Electrical Power and Energy Systems*, *134*. https://doi.org/10.1016/j.ijepes.2021.107425
[26] Satpathy, P. K., Das, D., & Dutta Gupta, P. B., (2004), Critical switching of capacitors to prevent voltage collapse, *Electric Power Systems Research*, *71*(1), 11–20. https://doi.org/10.1016/j.epsr.2003.12.016
[27] Vanfretti, L., & Arava, V. S. N., (2020), Decision tree-based classification of multiple operating conditions for power system voltage stability assessment, *International Journal of Electrical Power and Energy Systems*, *123*, 1–9. https://doi.org/10.1016/j.ijepes.2020.106251
[28] Razmi, H., Shayanfar, H. A., & Teshnehlab, M., (2012), Steady state voltage stability with AVR voltage constraints, *International Journal of Electrical Power and Energy Systems*, *43*(1), 650–659. https://doi.org/10.1016/j.ijepes.2012.06.051
[29] Perninge, M., & Söder, L., (2011), Risk estimation of the distance to voltage instability using a second order approximation of the saddle-node bifurcation surface, *Electric Power Systems Research*, *81*(2), 625–635. https://doi.org/10.1016/j.epsr.2010.10.021
[30] Dobson, I., & Chiang, H. D., (1989), Towards a theory of voltage collapse in electric power systems, *Systems and Control Letters*, *13*(3), 253–262. https://doi.org/10.1016/0167-6911(89)90072-8
[31] Church, C., Morsi, W. G., Diduch, C. P., El-Hawary, M. E., & Chang, L., (2010), Voltage collapse detection using ant colony optimization for smart grid applications, *EPEC 2010 - IEEE Electrical Power and Energy Conference: "Sustainable Energy for an Intelligent Grid."* https://doi.org/10.1109/EPEC.2010.5697185
[32] Verbič, G., & Gubina, F., (2004), A novel scheme of local protection against voltage collapse based on the apparent-power losses, *International Journal of Electrical Power and Energy System*, *26*(5), 341–347. https://doi.org/10.1016/j.ijepes.2003.11.001
[33] Nizam, M., Mohamed, A., & Hussain, A., (2010), Dynamic voltage collapse prediction in power systems using support vector regression, *Expert Systems with Applications*, *37*(5), 3730–3736. https://doi.org/10.1016/j.eswa.2009.11.052
[34] Sanz, F. A., Ramirez, J. M., & Posada, J., (2016), Statistical method for on-line voltage collapse proximity estimation, *International Journal of Electrical Power and Energy Systems*, *82*, 392–399. https://doi.org/10.1016/j.ijepes.2016.03.035
[35] Al-Hinai, A., & Choudhry, T. M. A. C., (2001), Voltage Collapse Prediction for Interconnected Power Systems, In *Proc. of 33rd North American Power Symposium (NAPS), College Station, TX, October 2001*. College Station, TX. Retrieved from https://www.researchgate.net/publication/266450683
[36] Balamourougan, V., Sidhu, T. S., & Sachdev, M. S., (2004), A technique for real time detection of voltage collapse in power systems, *IEE Conference Publication*, *2*, 639–642. https://doi.org/10.1049/cp:20040205
[37] Pourjafari, E., & Mojallali, H., (2011), Predictive control for voltage collapse avoidance using a modified discrete multi-valued PSO algorithm, *ISA Transactions*, *50*(2), 195–200. https://doi.org/10.1016/j.isatra.2010.12.006
[38] Wang, Y., Xu, Q., & Zheng, J., (2020), The new steady state voltage stability analysis methods with computation loads separation technique in DC power systems, *International Journal of Electrical Power and Energy Systems*, *115*, 1–8. https://doi.org/10.1016/j.ijepes.2019.105482
[39] Li, X., Zhang, L., Jiang, T., Li, F., Chen, H., & Jia, H., (2021), Relaxed decoupled direct calculation of voltage collapse points and its application in static voltage stability region boundary formation, *International Journal of Electrical Power and Energy Systems*, *125*, 1–13. https://doi.org/10.1016/j.ijepes.2020.106452
[40]Šmon, I., Pantoš, M., & Gubina, F., (2008), An improved voltage-collapse protection algorithm based on local phasors, *Electric Power Systems Research*, *78*(3), 434–440. https://doi.org/10.1016/j.epsr.2007.03.012
[41] Liu, S., Shi, R., Zhang, T., Tang, F., Zhang, L., Liu, L., … Zhang, M., (2021), An integrated scheme for static voltage stability assessment based on correlation detection and random bits forest, *International Journal of Electrical Power and Energy Systems*, *130*, 1–10. https://doi.org/10.1016/j.ijepes.2021.106898
[42] Yang, F., Ling, Z., Wei, M., Mi, T., Yang, H., & Qiu, R. C., (2021), Real-time static voltage stability assessment in large-scale power systems based on spectrum estimation of phasor measurement unit data, *International Journal of Electrical Power and Energy Systems*, *124*, 1–10. https://doi.org/10.1016/j.ijepes.2020.106196
[43] Ratra, S., Tiwari, R., & Niazi, K. R., (2018), Voltage stability assessment in power systems using line voltage stability index, *Computers and Electrical Engineering*, *70*, 199–211. https://doi.org/10.1016/j.compeleceng.2017.12.046
[44] Chandra, A., & Pradhan, A. K., (2019), Online voltage stability and load margin assessment using wide area measurements, *International Journal of Electrical Power and Energy Systems*, *108*, 392–401. https://doi.org/10.1016/j.ijepes.2019.01.021
[45] Yang, H., Qiu, R. C., Shi, X., & He, X., (2020), Unsupervised feature learning for online voltage stability evaluation and monitoring based on variational autoencoder, *Electric Power Systems Research*, *182*(4), 1–13.

https://doi.org/10.1016/j.epsr.2020.106253
[46] Alzaareer, K., Saad, M., Mehrjerdi, H., Ziad El-Bayeh, C., Asber, D., & Lefebvre, S., (2020), A new sensitivity approach for preventive control selection in real-time voltage stability assessment, *International Journal of Electrical Power and Energy Systems*, *122*, 1–10. https://doi.org/10.1016/j.ijepes.2020.106212
[47] Rodriguez-Garcia, L., Perez-Londono, S., & Mora-Florez, J., (2019), An optimization-based approach for load modelling dependent voltage stability analysis, *Electric Power Systems Research*, *177*. https://doi.org/10.1016/j.epsr.2019.105960
[48] Painuli, S., Singh Rawat, M., Vadhera, S., & Tamta, R., (2018), Comparison of Line Voltage Stability Indices for Assessment of Voltage Instability in high Voltage Network, In *1st International Conference on New Frontiers in Engineering, Science & Technology* (pp. 819–825). New Delhi, India. Retrieved from https://www.researchgate.net/publication/322569809
[49] Ramírez Perdomo, S. L., & Lozano, C. A. M., (2014), Evaluation of indices for voltage stability monitoring using PMU measurements, *Ingenieria e Investigacion*, *34*(3), 44–49. https://doi.org/10.15446/ing.investig.v34n3.43002